Star Formation and AGNs

- Jorge Díaz; IATE.
- Carlos Donzelli; IATE.
- Nelson Padilla; PUC, Ch.
- Hitoshi Hanami; Iwate University, Jp.
- Naofumi Fujishiro; Kyoto SU, Jp.
- Masayuki Akiyama; Tohoku University, Jp.
- Tomohiro Yoshikawa, Kyoto SU, Jp.
- Toshinobu Takagi, ISAS, Jp.

Evolution of Star Formation Density

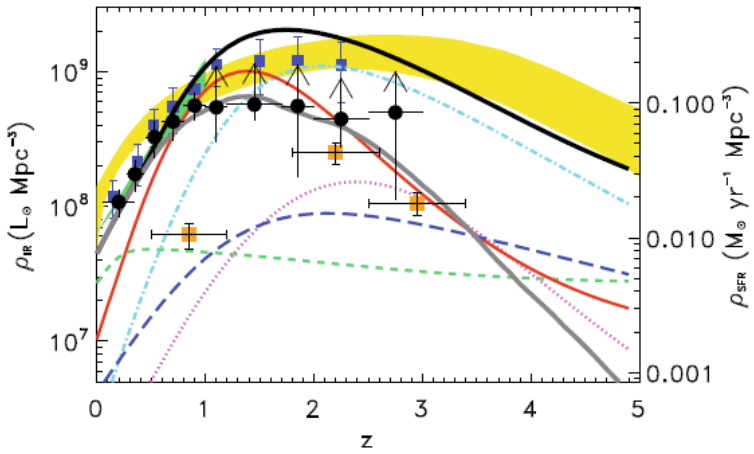

Fig. 4. Evolution of the total IR LD (or SFD) with z. The results of integrating our observed total IR LF in each z-bin are shown as black filled circles. The 3σ best-fitting envelope to the Hopkins & Beacom (2006) data collection from different surveys (yellow area), the results of Le Floc'h et al. (2005) and Rodighiero et al. (2010) as total IR LD up to $z \sim 1$ (green area) and $z \sim 2.5$ (blue filled squares), respectively, and the contribution to the SFD of radio detected sub-mm sources (orange filled squares) from Chapman et al. (2005) are also reported. The differently coloured lines are the GP2010 model predictions in terms of total IR LD (black solid), IR LD to the PEP luminosity completeness limit (grey solid), and single contributions from the different IR populations

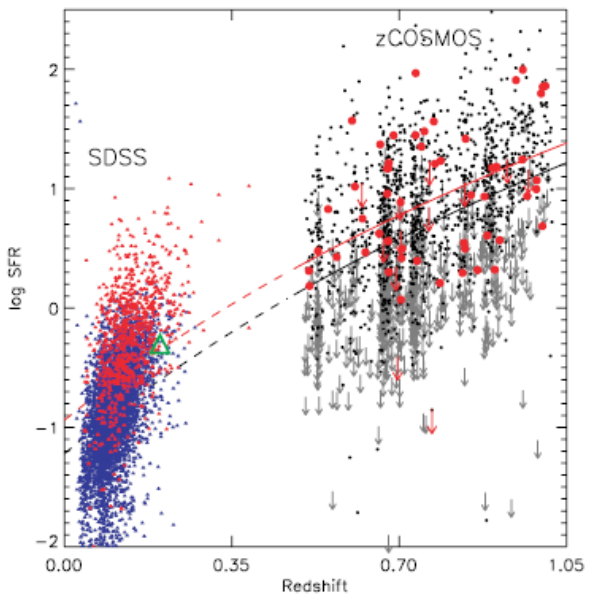

Figure 10. Cosmic evolution of star formation. At $z > 0.48$, we show the SFR-z distribution for all zCOSMOS galaxies with $\log M > 10.6$ (small black circles and gray arrows) and those hosting AGN with $\log L_X > 42$ (73; large red circles and arrows). The best-fit linear relation for zCOSMOS galaxies, including those with upper limits, is shown for both populations (black: galaxies; red: AGN hosts) with an extrapolation to lower redshifts (dashed lines). For comparison, we plot SFRs of AGN hosts from the SDSS with an equivalent selection on stellar mass; obscured AGNs (type 2) from the sample of Kauffmann et al. (2003b) are shown with strong AGNs ($\log L_{O\,III} > 40.5$) in red and those of lower luminosity in blue. A large green triangle marks the mean value of the SFR for the SDSS type 1 AGNs (Kim et al. 2006).

Rest frame IR 8um-1000um LD of galaxies and AGNs up to z=3. Gruppioni et al. 2010

SFRs and AGNs evolve with z. Silverman et al. 2009

Bimodal Distribution, the green valley and AGNs.

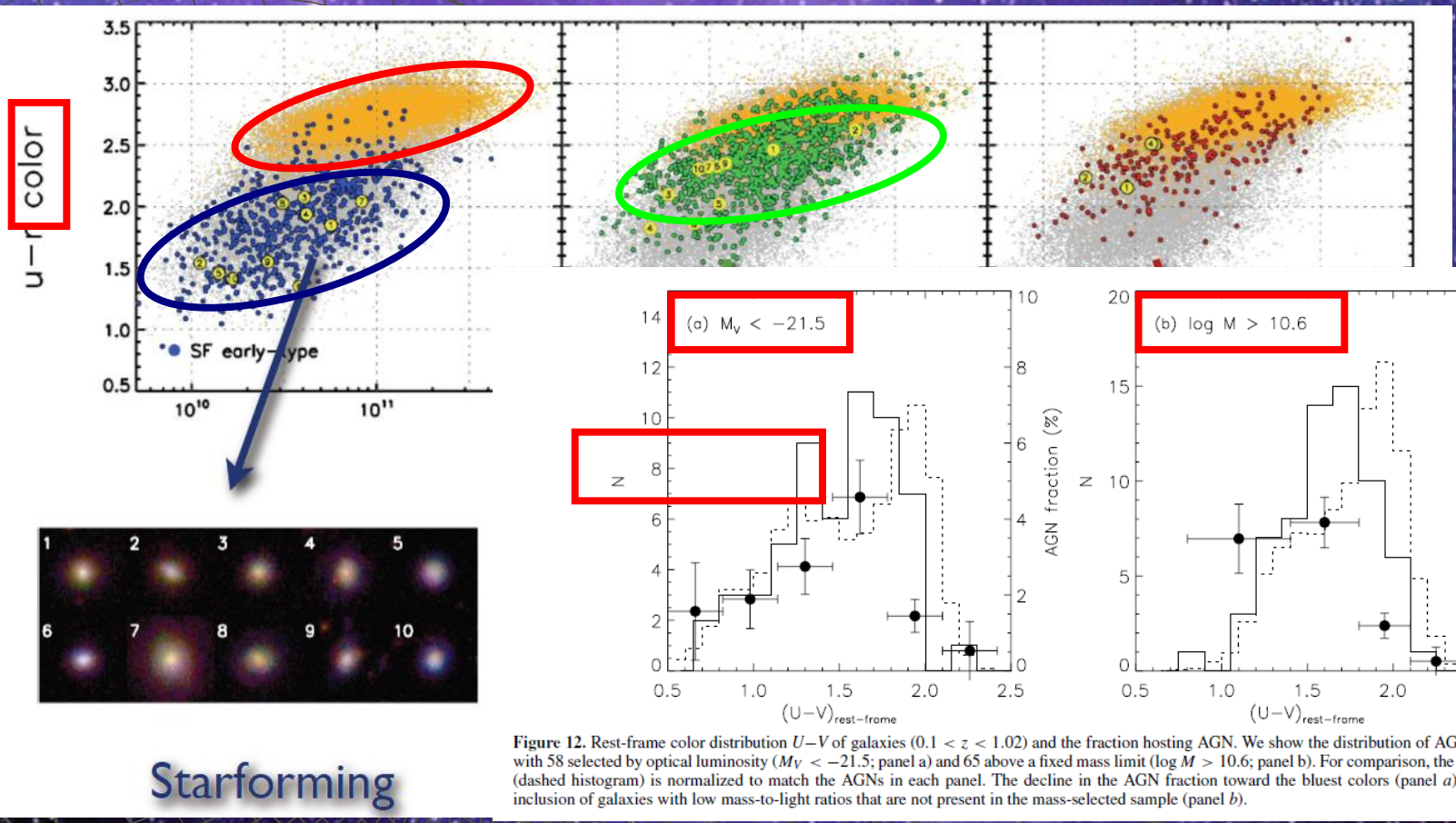

Figure 12. Rest-frame color distribution $U-V$ of galaxies ($0.1 < z < 1.02$) and the fraction hosting AGN. We show the distribution of AGN hosts (solid histogram) with 58 selected by optical luminosity ($M_V < -21.5$; panel a) and 65 above a fixed mass limit ($\log M > 10.6$; panel b). For comparison, the parent galaxy distribution (dashed histogram) is normalized to match the AGNs in each panel. The decline in the AGN fraction toward the bluest colors (panel *a*) appears to be due to the inclusion of galaxies with low mass-to-light ratios that are not present in the mass-selected sample (panel *b*).

Migration from SF to RS by AGN phase. Schawinski et al. 2009

The fraction of AGN peak up in the green valley for both Luminosity and Mass. Silverman et al. 2009

Finding AGNs:

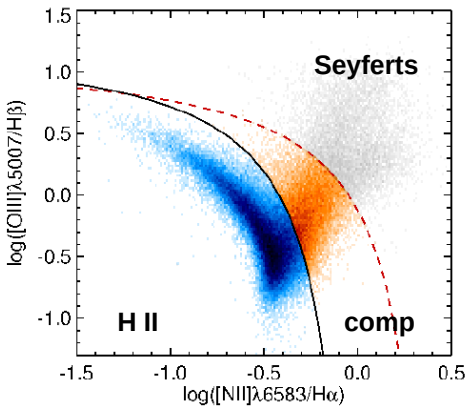

Fig. 2. Log([N II]/Hα) vs log([O III] λ5007/Hβ) BPT diagram. Solid line show the Kauf03 empirical division between SF and composite galaxies, and dashed line represents the Kew01 starburst limit. [See the electronic edition of the Journal for a color version of this figure.]

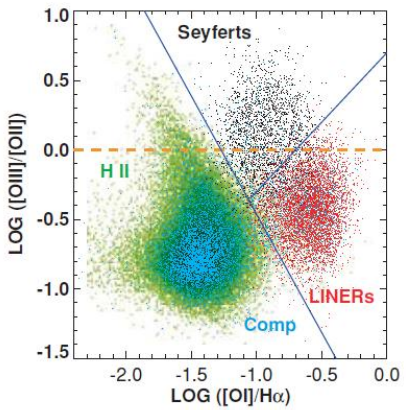

Figure 5. The [O III]/[O II] versus [O I]/Hα diagnostic diagram for SDSS galaxies with S/N > 3. Galaxies have been classified using the standard BPT diagnostic diagrams (Fig. 4). Ambiguous galaxies are not included. Our new preferred classification scheme is shown in blue. The H80 LINER line (orange dashed) is also shown.

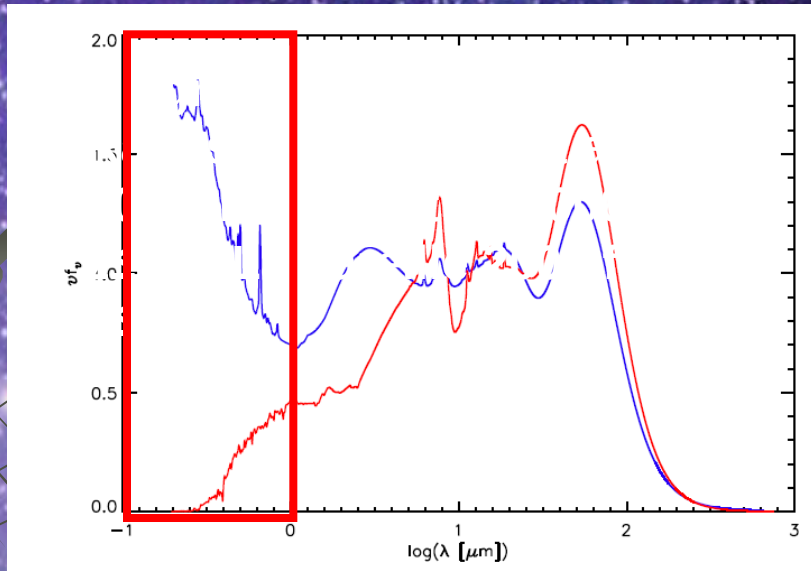

Fig. 4.— Averaged modeled SEDs of type-1 (blue) and type-2 (red) quasars. The spectra are normalized at 24 μm. We plot νf_ν to highlight the differences between the two.

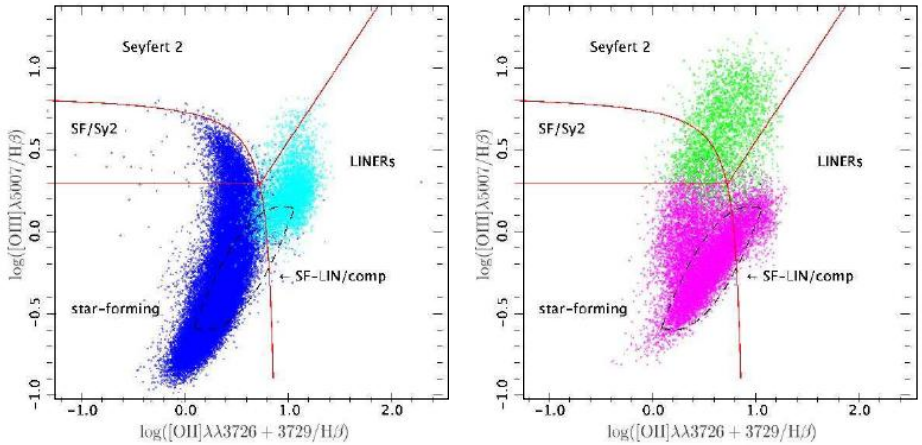

Figure 4. This is the new improved "blue" classification of emission-line galaxies. The two diagnostic diagrams show the relation between two line ratios: log([OIII]λ 5007/Hβ) vs. log([OII]$\lambda\lambda$3726+3729/Hβ). According to the red classification (see Fig. 2), star-forming galaxies are shown in blue, LINERs in cyan, composites in magenta, and Seyfert 2 in green. For clarity, the two first classes are shown only in the left panel, while the two last classes are shown only in the right panel. The red curves show the new empirical separations defined in the text: between star-forming galaxies and AGNs (Eq. 1), between Seyfert 2 and LINERs (Eq. 4), between star-forming galaxies and SF/Sy2 (Eq. 2). The black dashed curves delimits the region where lies the majority of composites (SF-LIN/comp region, Eq. 3).

But there are Obscured AGNs, detectable only in MIR wavelengths, mainly Seyfert-2. Hiner et al 2009

Finding AGNs

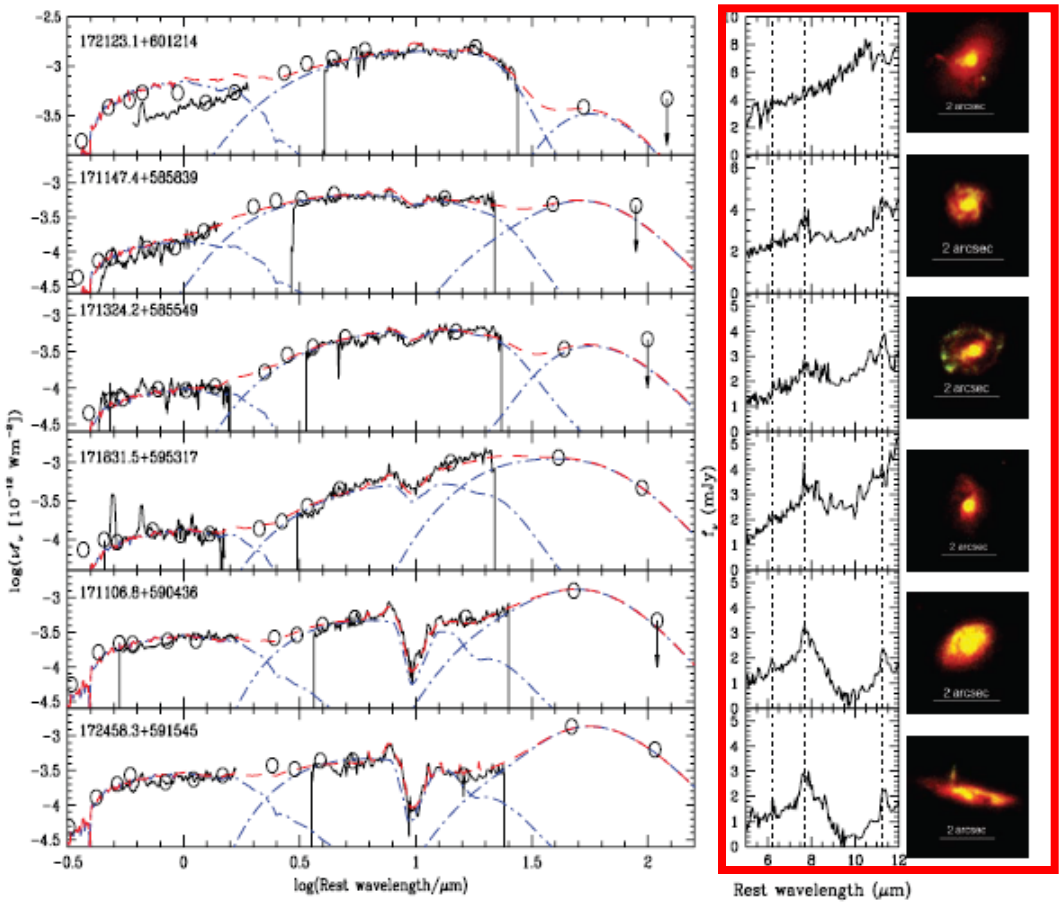

FIG. 2.—SEDs and *HST* images of the six type 1 quasars, in order of increasing silicate absorption. The solid black lines are the IRTF Spex and *Spitzer* IRS spectra (both smoothed to reduce noise) and the black open circles photometry from SDSS, IRTF, and *Spitzer*. The model fit is shown as the red dashed line, with (*from left to right*) the stellar component, hot dust component (including absorption, but excluding PAH emission), and sum of warm and cold dust components shown as blue dash-dotted lines. To the right of the SEDs we show expanded plots of the IRS spectra around the PAH wavelengths. The ACS images have the long-wavelength image colored red, and the short-wavelength image in green.

AGNs SED is affected by dusty starforming disc. Lacy et al 2007

Photometric Database

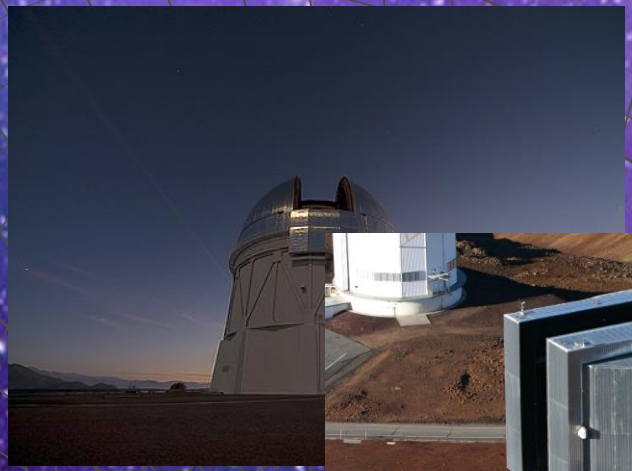

u band, Blanco 4m,
CTIO

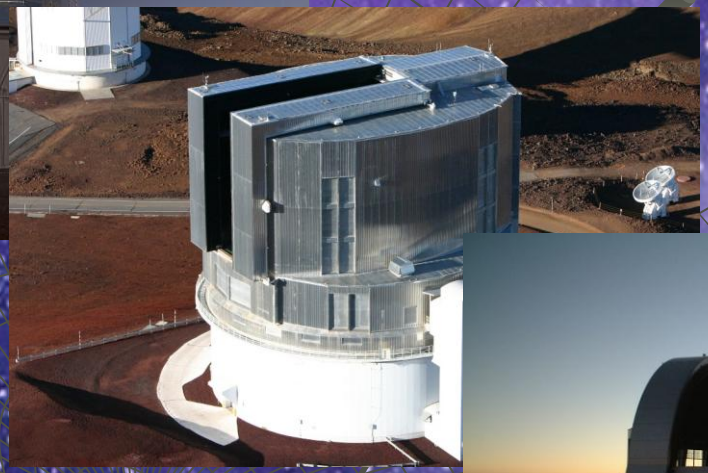

B, V, R, i, z bands, Subaru 8.2m,
NAOJ

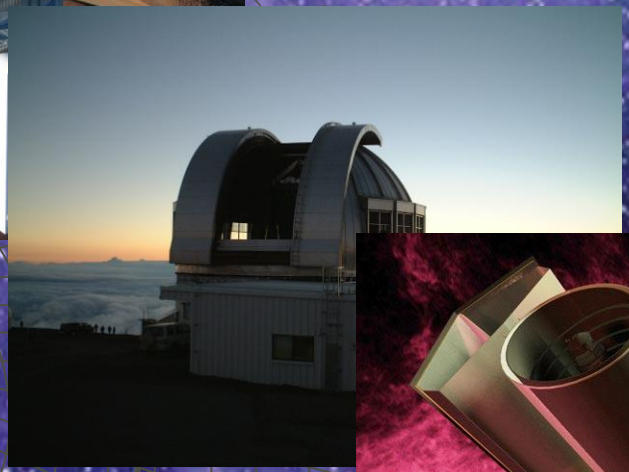

J, H, K bands, UKIRT 3.8m,
JAC

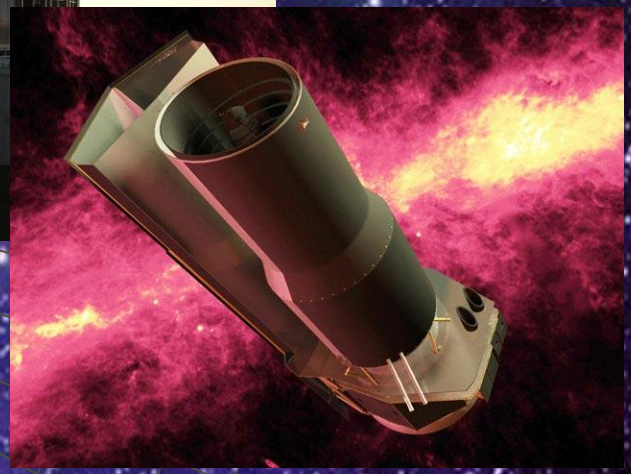

I1, I2, I3, I4, M1, M2, M3 bands, IRAC/MIPS
Spitzer, NASA

Color-color diagrams: looking for Balmer break

uBV diagram for z>0.25

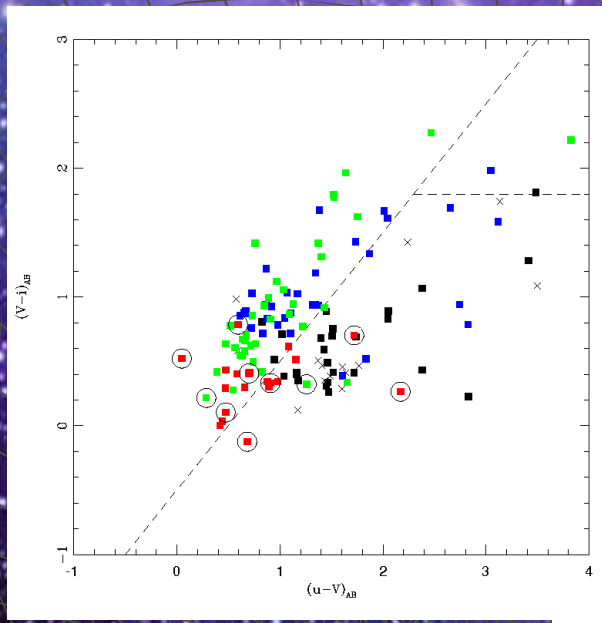

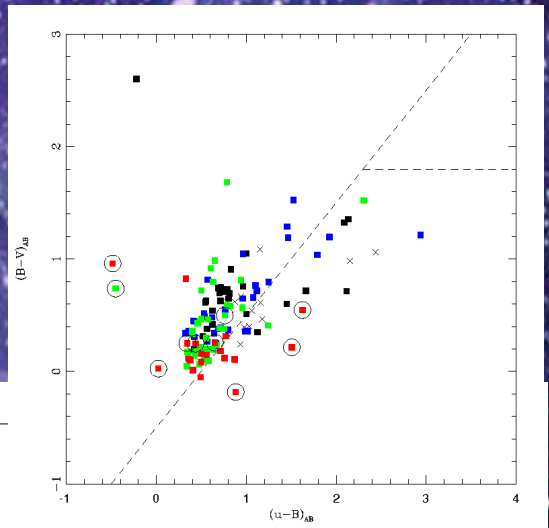

uVi diagram for z>0.5

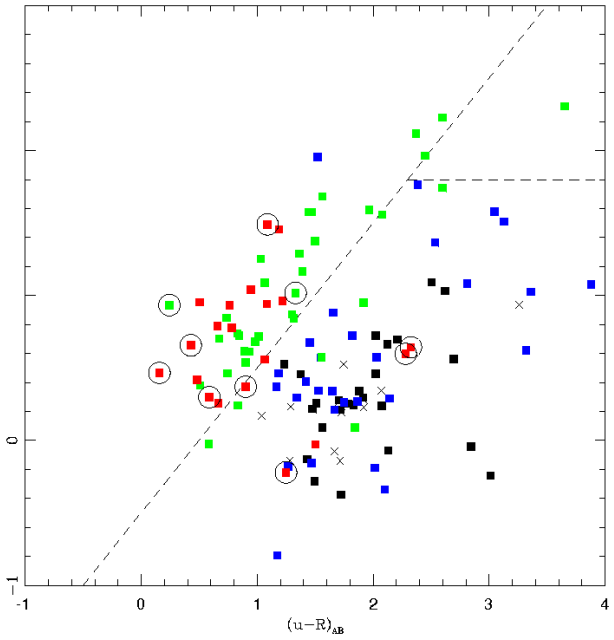

uRJ diagram for z>0.75

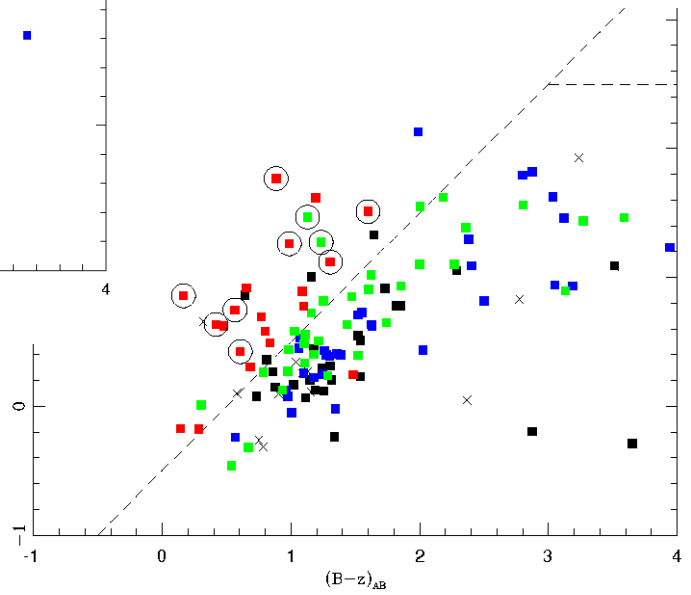

BzK diagram to pick up high-z galaxies (z>1.25), Daddi et al 2004

Spectroscopic Data

_1 mask, 220 slits, ~5h,
IMACS/Magellan 6.5m, LCO

_3 masks, x~55 slits, x~7h,
GMOS/GEMINI South 8m, GO

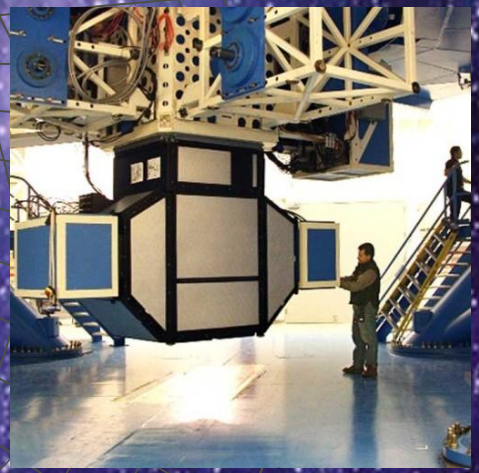

Slit masks

Magellan FOV: 26’x26’

Gemini FOV: 5’x5’

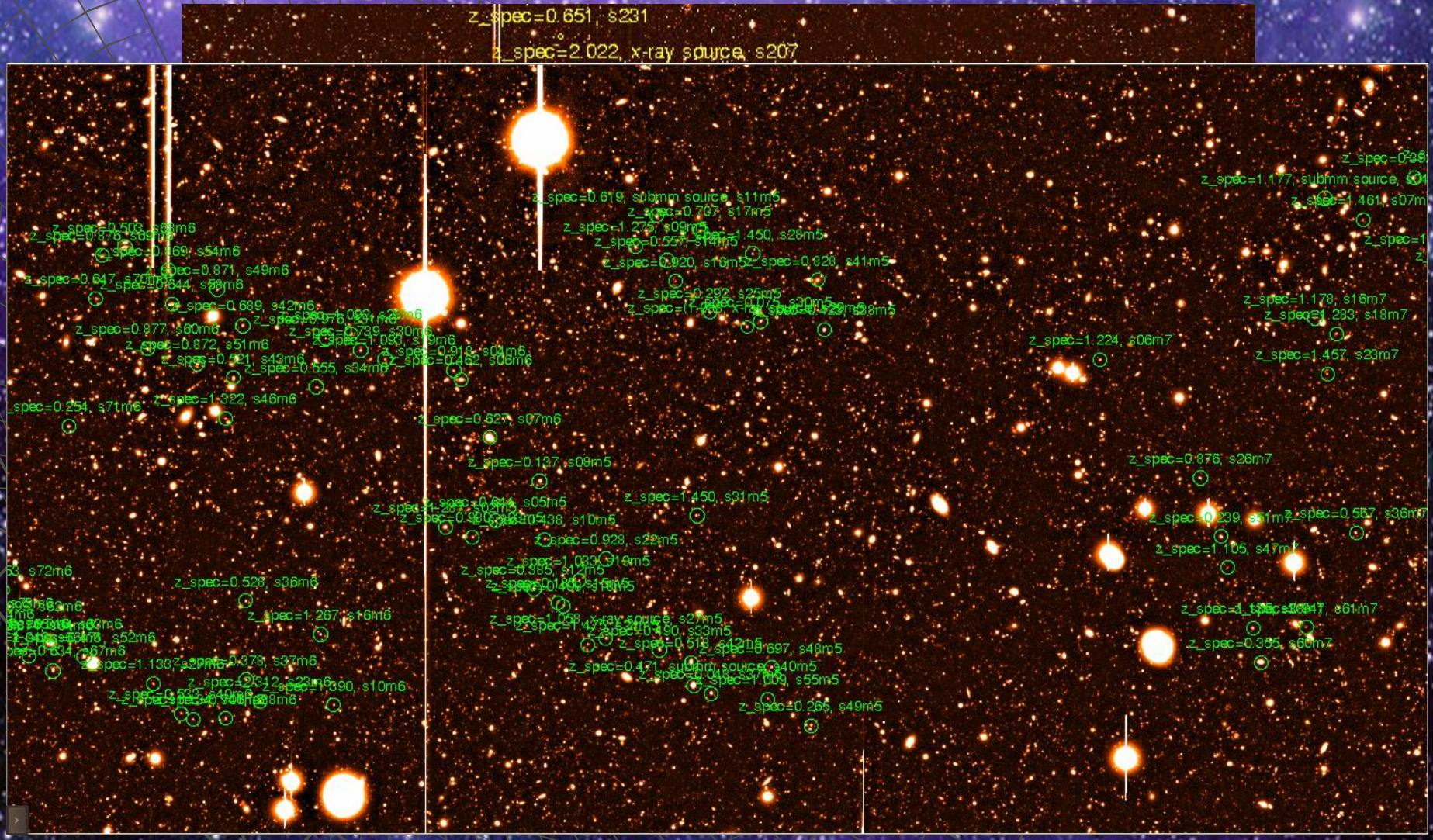

Some results

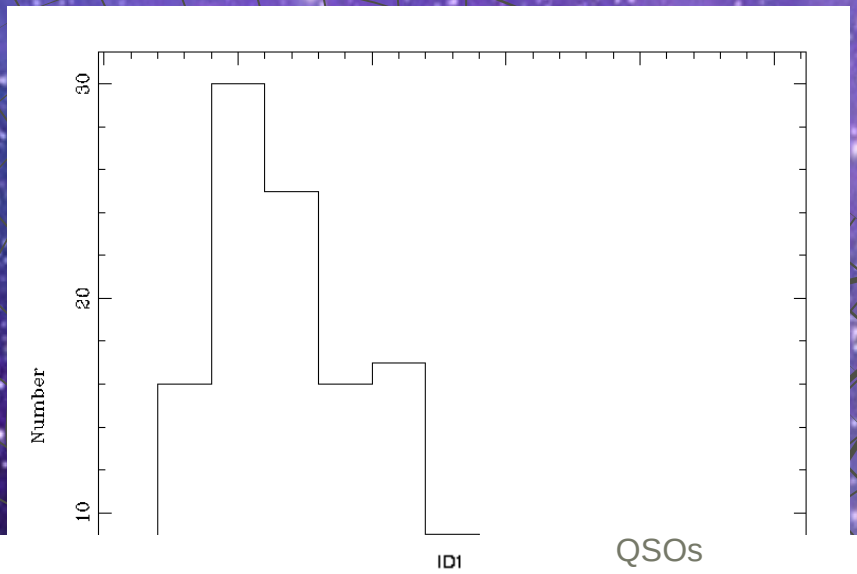

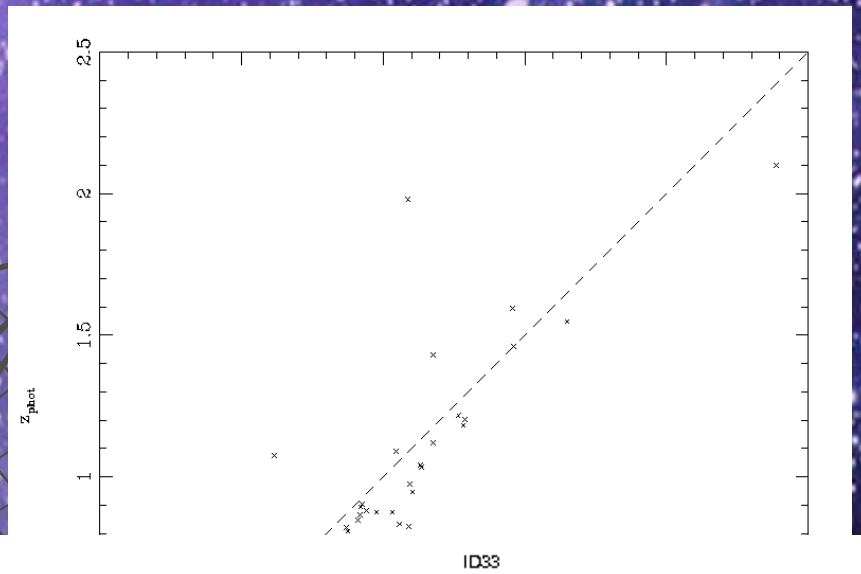

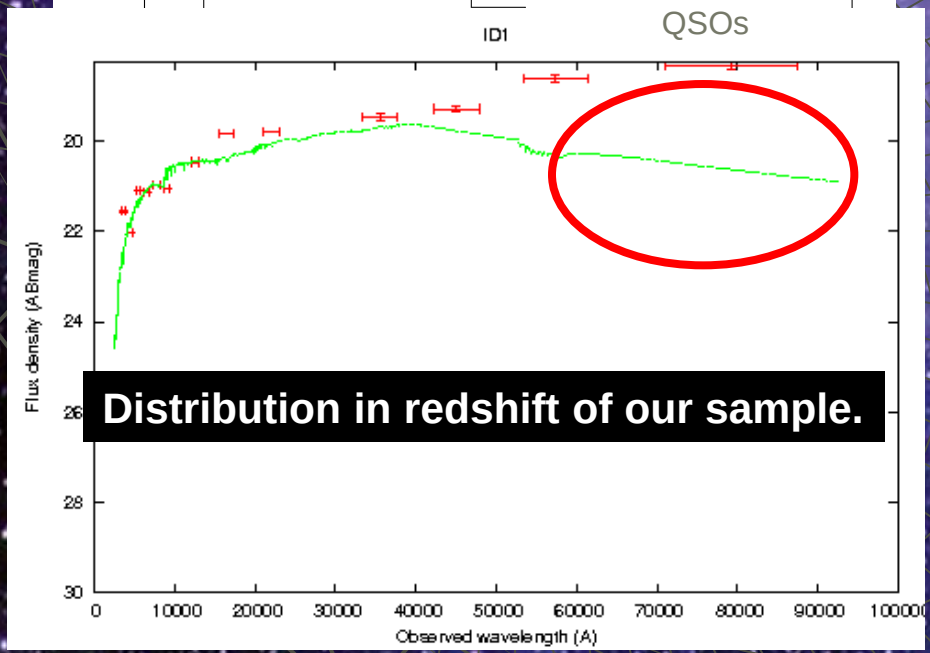

Distribution in redshift of our sample.

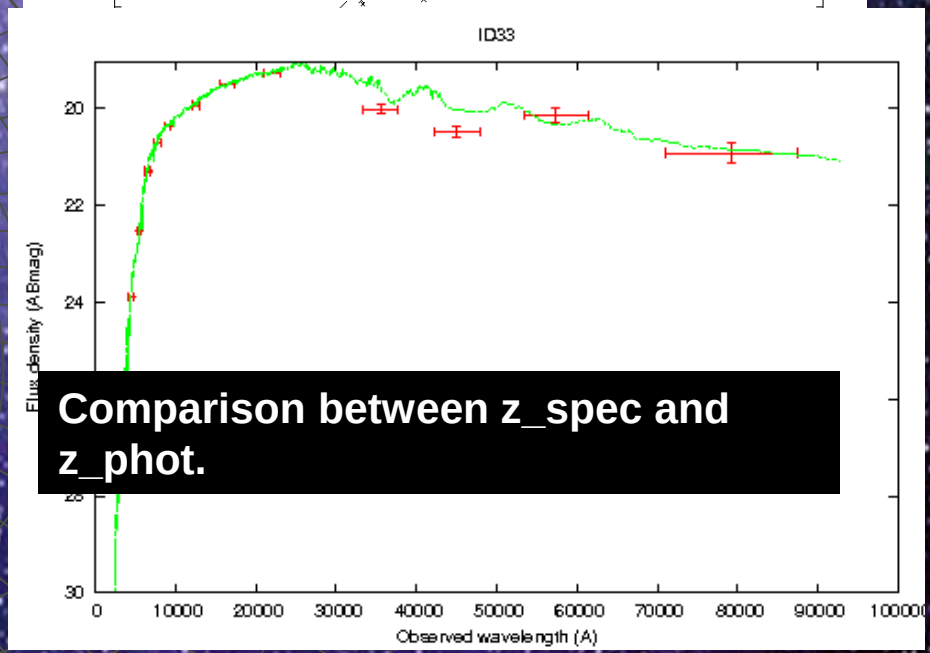

Comparison between z_spec and z_phot.

AGN indetification

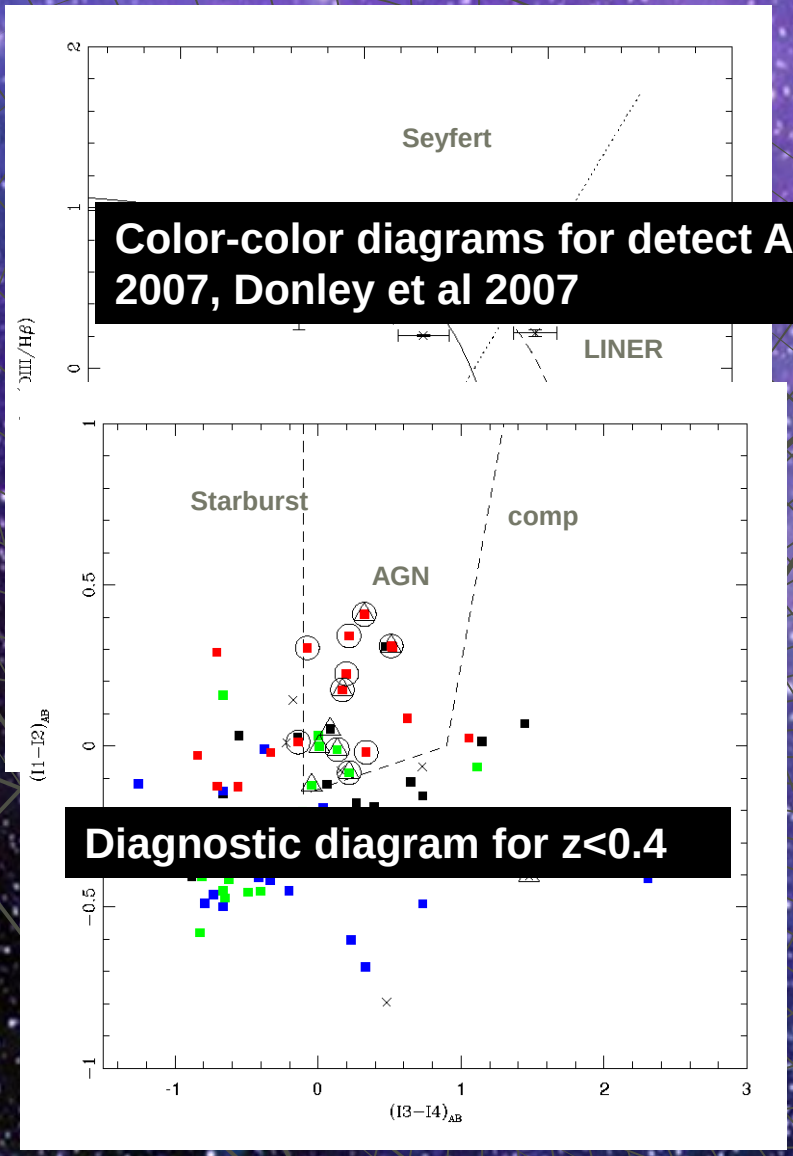

Color-color diagrams for detect AGNs using IRAC Spitzer bands. Lacy et al 2007, Donley et al 2007

Diagnostic diagram for z<0.4

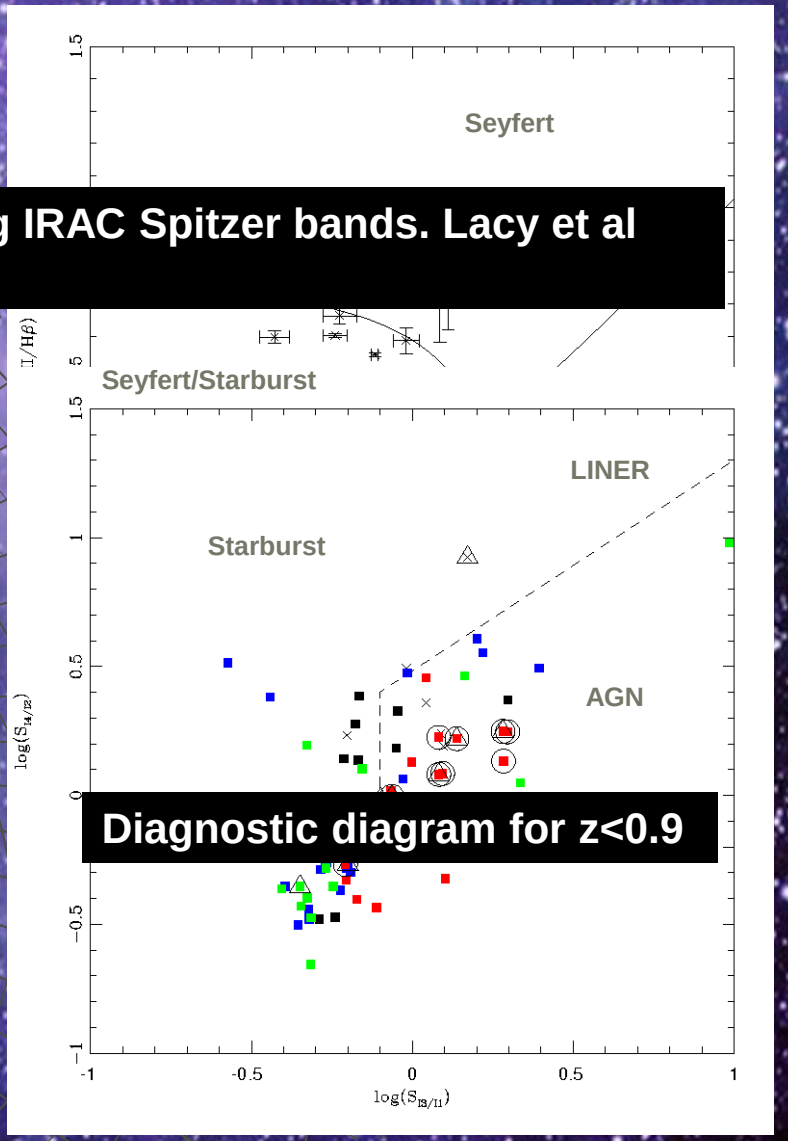

Diagnostic diagram for z<0.9

Ongoing Work

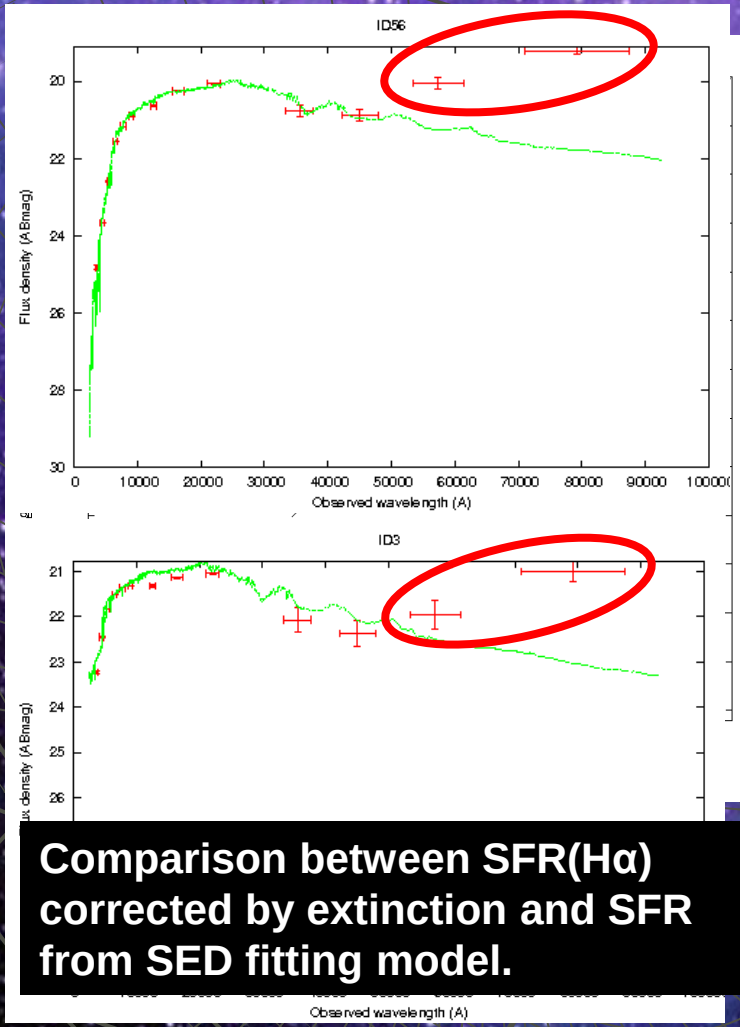

Comparison between SFR(Hα) corrected by extinction and SFR from SED fitting model.

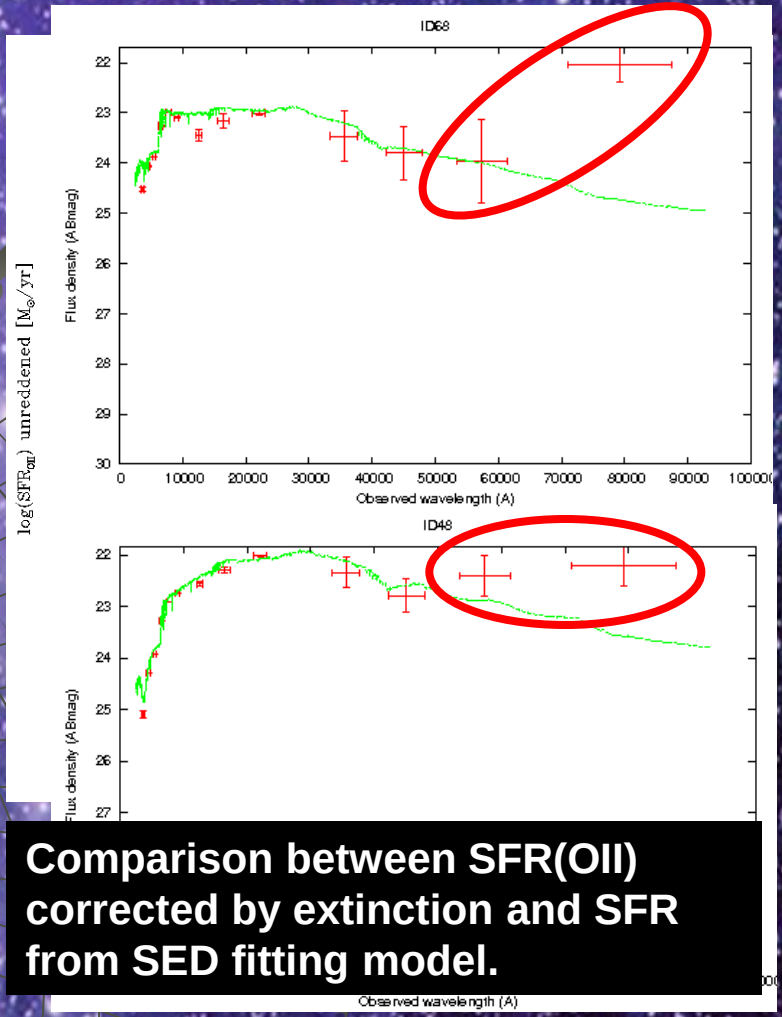

Comparison between SFR(OII) corrected by extinction and SFR from SED fitting model.

SED fitting model underestimates the SFR considering only stellar component.

_ Are there hidden AGNs or dusty starburst component present?

Thank you

_To finish, good news?:

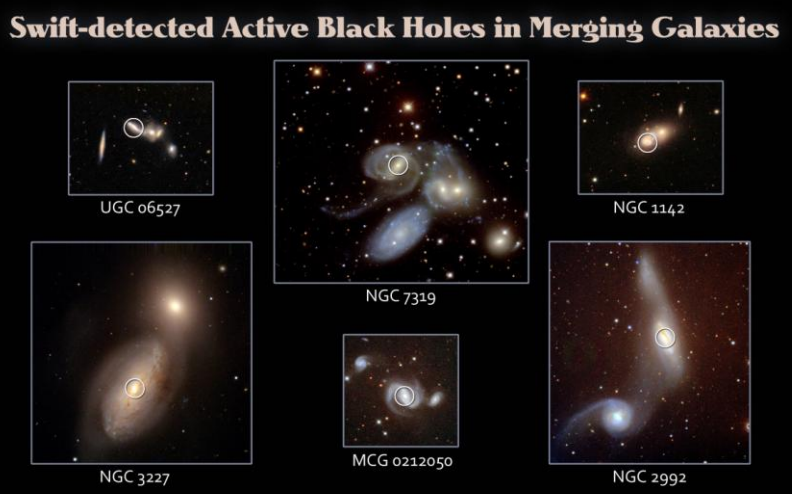

Koss et al 2010

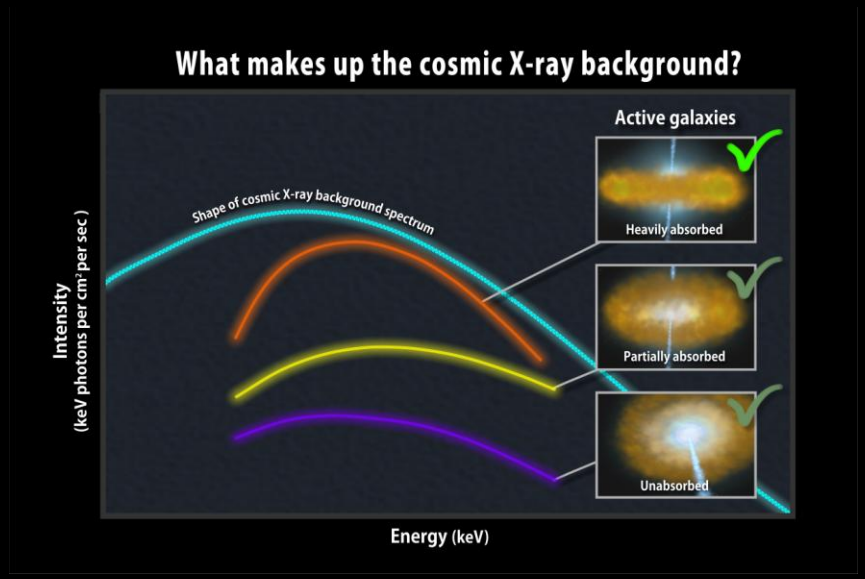

Burlon et al. 2010